Extension of Equivalent Angle-of-Attack Method for Nonlinear Flowfields

M.J. Hemsch* and J.N. Nielsen†
Nielsen Engineering & Research, Inc., Mountain View, California

Recent experimental results show that the control effectiveness of a missile fin in supersonic flow at moderate to high angles of attack is a strong nonlinear function of freestream Mach number, body incidence angle, fin bank angle, and fin deflection angle. Analysis of the experimental results using an Euler finite-difference computer code with flow separation, together with the equivalent angle-of-attack concept, indicates that the observed nonlinearities are due to the variation of local dynamic pressure and local Mach number around the missile body alone. The nonlinearities are shown to be a strong source of control cross-coupling for high Mach number, high angle-of-attack combinations. The analysis suggests a relatively simple yet comprehensive approach for accurately accounting for these nonlinear effects. The impact of the results on missile aeroprediction methods is discussed.

Nomenclature

a = body radius
AR = aspect ratio of wing alone
$C_{N_{F(B),i}}$ = normal-force coefficient of fin i in the presence of a circular body, referenced to fin planform area
C_{N_W} = normal-force coefficient of wing alone
D = body diameter
K_W = Beskin upwash factor
K_ϕ = sideslip factor
M_c = cross flow Mach number, $M_\infty \sin\alpha_c$
M_ℓ = Mach number at a point in the body flowfield
$\bar{M}_\ell$ = local Mach number in presence of body alone averaged over exposed span of fin [Eq. (5)]
M_∞ = freestream Mach number
q_ℓ = dynamic pressure at a point in the body flowfield
$\bar{q}_\ell$ = local dynamic pressure in presence of body alone averaged over exposed span of fin [Eq. (4)]
q_∞ = dynamic pressure of the freestream
s_m = semispan of fin
V_∞ = freestream velocity
x/D = distance aft of nose tip in (cylindrical) body diameters
α = angle of attack
α_c = angle between body axis and wind velocity vector
α_{eq_i} = equivalent angle of attack of fin i; i.e., angle of attack of wing alone which gives same normal-force coefficient as that of fin i
$\hat{\alpha}_{eq_i}$ = equivalent angle of attack of fin i if all fins are undeflected
δ_i = deflection of fin i, positive when the leading edge is rotated toward the leeward side of the body
$(\Delta\alpha)_{v_i}$ = average angle of attack induced on fin i by vortices
λ = fin taper ratio
Λ_{ji} = fin deflection factor
ϕ = roll angle of fin i measured from the horizontal plane, positive windward

Presented as Paper 83-2083 at the AIAA Atmospheric Flight Mechanics Conference, Gatlinburg, Tenn., Aug. 15-17, 1983; received Oct. 20, 1983; revision received Feb. 16, 1984.

*Manager, Missile Aerodynamics. Associate Fellow AIAA. Currently with Kentron International, Hampton, Va.

†Chief Scientist. Fellow AIAA. Currently Chief Scientist of NASA/Ames Research Center.

Introduction

RECENTLY, engineering methods have been developed for estimating fin (or wing) forces and moments in the presence of a missile body and other fins with sufficient accuracy to predict lateral and control characteristics up to high angles of attack.[1-4] The methods use systematic data bases, vortex tracking and the equivalent angle-of-attack (α_{eq}) concept.

It is the purpose of this paper first to present experimental results[5] which show that the control effectiveness of a missile fin in supersonic flow at moderate to high angles of attack is a strong nonlinear function of freestream Mach number, body incidence angle, fin bank angle and fin deflection angle, second to show that the observed nonlinearities are a strong source of control cross-coupling for high Mach number, high angle-of-attack combinations, and third to demonstrate with the help of a Euler code and the α_{eq} concept that the observed nonlinearities are due to the variation of local dynamic pressure and local Mach number around the body alone. Finally, a simple but comprehensive approach is presented for accurately accounting for the nonlinearities and the impact of the results on missile aeroprediction methods is discussed.

Review of the α_{eq} Concept

It will be convenient for the discussion in the following sections to review the α_{eq} concept.[3] The concept is used to estimate the nonlinear force and moment coefficients of fins mounted on bodies by relating the fin coefficients to those of a wing alone composed of two of the same fins joined at their root chords. The α_{eq} for fin i is obtained from solution of the equation

$$C_{N_W}(\alpha_{eq_i}) = C_{N_{F(B),i}}[\alpha_c, \phi_i, \delta_{1-4}, a/s_m, (\Delta\alpha)_{v_i}] \quad (1)$$

Equation (1) by itself is not very useful. What is needed is a way to relate the parameters in the argument lists of the functions so that a change in one or more of the parameters can be related to a change in α_{eq} and hence to a change in $C_{N_{F(B)}}$. Using the notion of "average" velocity components seen by the fin of interest (fin i) and drawing extensively on slender-body theory, we derived in Ref. 3 the following relationships:

$$\tan\hat{\alpha}_{eq_i} = K_W \tan\alpha_c \cos\phi_i + \frac{4}{AR} K_\phi \tan\alpha_c \sin\alpha_c \sin\phi_i \cos\phi_i + \tan(\Delta\alpha)_{v_i} \quad (2)$$

and

$$\alpha_{eq_i} = \hat{\alpha}_{eq_i} + \sum_{j=1}^{4} \Lambda_{ji}\delta_j \qquad (3)$$

The assumptions involved in the derivation of Eqs. (2) and (3) and a discussion of the many uses of the approach are given in the reference. Note that for the purposes of the discussion to follow that it is implicit in the α_{eq} concept as set forth in Ref. 3 that the local dynamic pressure and local Mach number in the region occupied by a fin do not differ significantly from the freestream values. For these conditions and the assumptions of slender-body theory, Λ_{ji} is dependent only on the fin span-to-body diameter ratio.

Review of the Data

The data which will be presented were obtained with the model shown in Fig. 1. Only one fin (fin 2) was deflected. The fins have clipped delta planforms with a wing-alone aspect ratio of 2 and a taper ratio of 0.5. The airfoil section is a symmetric double wedge with a uniform thickness-to-chord ratio of 6%. The span-to-body diameter ratio is 2. The wing-alone curves to be used for the discussion are given in Fig. 2 and are taken from Ref. 6. The wings used to obtain the data given in Fig. 2 have modified double wedge airfoil sections.

Typical normal-force coefficient data are presented as a function of bank angle in Fig. 3 for the deflected fin for a body incidence angle of 20 deg. There are three features which should be noted. First, for the zero deflection curves, the maximum value of the normal-force coefficient is displaced

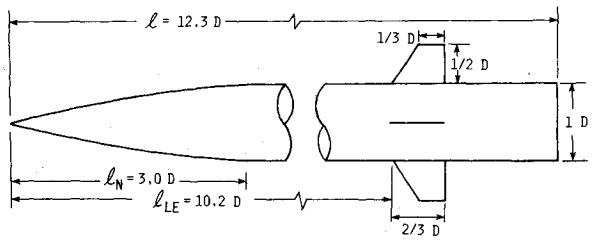

Fig. 1 Schematic of model used for control tests.

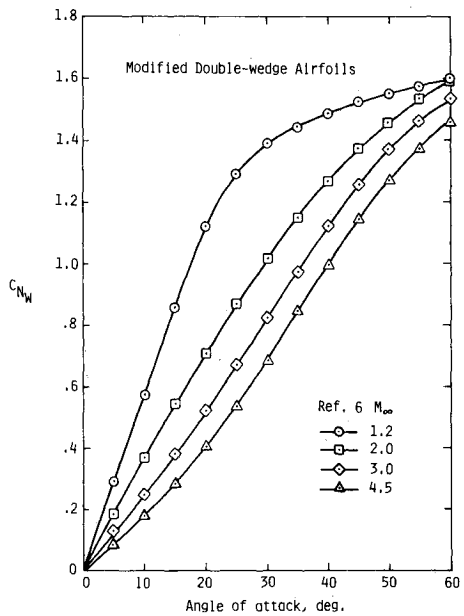

Fig. 2 Normal-force coefficient for $AR = 2$, $\lambda = 1/2$ clipped delta wing.

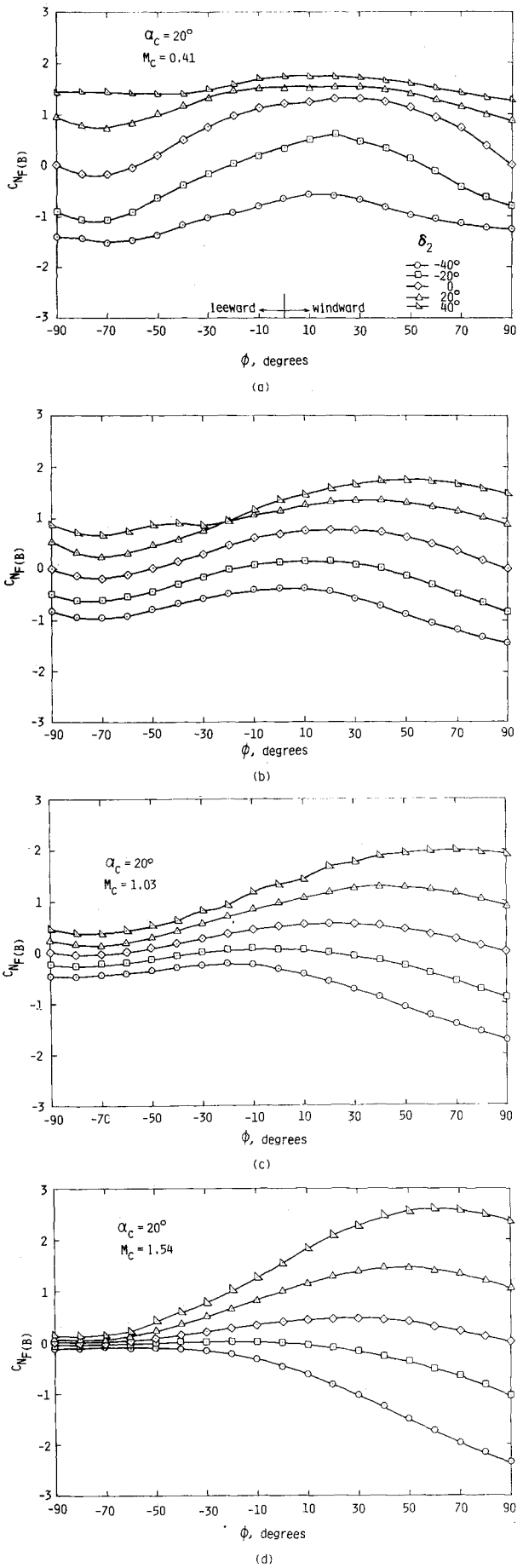

Fig. 3 Normal-force coefficient for deflected fin of $AR = 2$, $\lambda = 1/2$ mounted on body of Fig. 1: a) $M_\infty = 1.2$; b) $M_\infty = 2.0$; c) $M_\infty = 3.0$; d) $M_\infty = 4.5$.

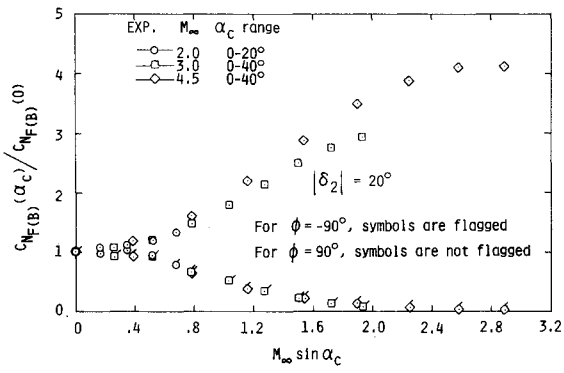

Fig. 4 Correlation of control effectiveness for leeward meridian and windward meridian fin positions.

toward the windward side of the body from the horizontal symmetry position of $\phi = 0$ to roughly $\phi = 25$ deg in accordance with slender-body theory (e.g., Ref. 3). Second, for the $M_\infty = 1.2$ data (Fig. 3a), positive fin deflection gives lower control effectiveness than negative fin deflection. This effect is due to the decrease in $dC_{N_w}/d\alpha$ with increasing α for the $M_\infty = 1.2$ wing-alone curves (Fig. 2). Third, the control effectiveness changes dramatically with increasing Mach number, decreasing for leeward bank angles and increasing for windward bank angles. In fact, for certain values of ϕ on the windward side, $C_{N_{F(B)}}$ is greater than the maximum value of 1.7 given by Hoerner[7] for a flat plate normal to the freestream.

A valuable perspective on the last phenomenon described above can be gained by plotting the fin normal-force coefficient for the $\phi = \pm 90$ deg positions as a function of cross-flow Mach number $M_c = M_\infty \sin\alpha_c$. This case represents control effectiveness since $C_{N_{F(B)}} = 0$ for $\phi = \pm 90$ deg and $\delta = 0$. The results are given in Fig. 4 for $M_\infty = 2.0$, 3.0, and 4.5 and fin deflection angles of ± 20 deg. The fin normal-force coefficient for a given α_c is normalized by its value at $\alpha_c = 0$ to give the curves a common value at $M_c = 0$. The $M_\infty = 1.2$ data are not shown to avoid cluttering the figure. However, for $M_\infty = 1.20$ and $\alpha_c \leq 20$ deg, the $C_{N_{F(B)}}(\alpha_c)/C_{N_{F(B)}}(0)$ ratio is within a few percent of unity. Figure 4 shows that the data correlate fairly well with cross-flow Mach number.

It is obvious from Fig. 4 that a yaw command in the "plus" configuration for a high cross-flow Mach number will lead to an induced rolling moment which must be answered by the horizontal fins. However, when a high-performance missile is pulling a high-g maneuver, much of the available horizontal fin deflection capability will be used to trim the vehicle in the pitch plane. Hence, little will be left to counter any induced rolling moment due to a yaw command. Clearly, this would put a limit on the α_c which the vehicle could safely reach for high cross-flow Mach numbers.

Analysis

The large variation in $C_{N_{F(B)}}$ with fin bank angle and the correlation of Fig. 4 prompts us to consider the local flowfield property variation (around the body alone). To do this we used the SWINT marching Euler solver[8] which has the capability of shedding and convecting vorticity at prescribed separation lines on the body. The separation line locations were determined from a correlation by Nielsen[9] made from Landrum's oil-flow data.[10] A series of runs was made on a three-caliber cone-cylinder for various Mach numbers and angles of attack.

For the purposes of the present work, we will use values of q_ℓ and M_ℓ which have been averaged over the exposed span of

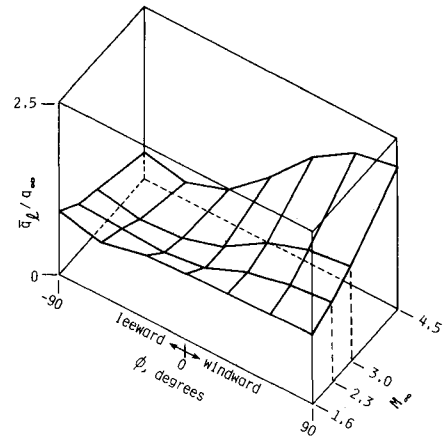

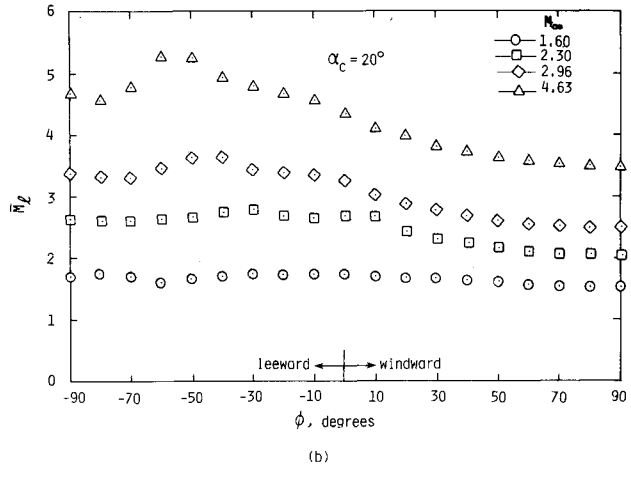

Fig. 5 Computed flowfield properties for a three-caliber cone-cylinder: a) average local dynamic pressure; b) average local Mach number.

fin, i.e.,

$$\bar{q}_\ell \equiv \frac{1}{s_m - a}\int_a^{s_m} q_\ell(\phi, r)\,dr \tag{4}$$

$$\bar{M}_\ell \equiv \frac{1}{s_m - a}\int_a^{s_m} M_\ell(\phi, r)\,dr \tag{5}$$

The averaging was applied along the radial line defined by the exposed fin span for $\delta = 0$ as if the fin were immersed in the body-alone flowfield. Hence, for the data presented here the integration interval was from a to $2a$. The computed results for $\bar{q}_\ell$ and $\bar{M}_\ell$ at 10 diameters aft of the nose tip for a body incidence angle of 20 deg are given in Fig. 5.

It is immediately apparent from the results shown in Fig. 5 that the variations of both the local Mach number and local dynamic pressure contribute to the behavior displayed in Figs. 3 and 4. At $M_\infty = 1.60$, for example, both $\bar{q}_\ell$ and $\bar{M}_\ell$ vary only slightly with ϕ from their freestream values. However, as M_∞ increases, the variation with ϕ of both quantities increases. At $M_\infty = 4.63$ and $\phi = 90$ deg, for instance, $\bar{q}_\ell/q_\infty = 2.07$ and $\bar{M}_\ell = 3.5$. Both of these flowfield values would contribute to values of $C_{N_{F(B)}}$ which are higher than expected when the fin is deflected, the lower Mach number giving a higher wing-alone normal-force coefficient slope.

Given the above results, it seems reasonable to conjecture that the wide variation in $C_{N_{F(B)}}$ seen in Fig. 3 is due to local flow field property variations caused by the presence of the body alone. This conjecture can be checked by using the equivalent angle-of-attack concept and the local flowfield property values of Fig. 5. Since only fin 2 of the model was

deflected we can write Eq. (3) as

$$\alpha_{eq_2} = \hat{\alpha}_{eq_2} + \Lambda_{22}\delta_2 \tag{6}$$

or

$$\Lambda_{22} = (\alpha_{eq_2} - \hat{\alpha}_{eq_2})/\delta_2 \tag{7}$$

If the conjecture is correct, it should be possible to use Eq. (7) to collapse the δ and ϕ dependence of the data in Fig. 3.

The steps which were used to check the conjecture for a given body angle of attack and freestream Mach number are as follows:

1) For a particular value of ϕ, determine $C_{N_{F(B)}}$ from the data for $\delta_2 = 0, \pm 20$ deg, ± 40 deg.

2) Multiply the results of step 1 by $q_\infty/\bar{q}_\ell$ for the particular value of ϕ to obtain $C_{N_{F(B)}}$ referenced to the (computed) local dynamic pressure.

3) Interpolate in the wing-alone curves of Fig. 2 (at the (computed) local Mach number) to obtain values of α_{eq} corresponding to the results of step 2. Ignore those data points which would require extrapolation of the wing-alone curves beyond $\alpha = 60$ deg.

4) Apply Eq. (7) to the results of step 3.

The results of the above procedure are given in Fig. 6. It was not possible to use SWINT for $M_\infty = 1.20$ because of subsonic flow on the windward side of the nose. But the computational results shown in Fig. 5 indicate that $\bar{q}_\ell \approx q_\infty$ and $\bar{M}_\ell \approx M_\infty$ for all bank angles. Thus, for the results of Figure 6a, step 2 was eliminated and $\bar{M}_\ell$ was set equal to M_∞.

The overall results of Fig. 6 indicate that the conjecture is correct. For $M_\infty = 1.20$ (Fig. 6a), all the large deviations occur when the fin is operating in the stall region, i.e., when $|\alpha_{eq}| > 22$ deg. We pointed out in Ref. 3 that although the α_{eq} concept can be used to obtain rough estimates of forces and moments for fins in the stall region, fin sweep due to a combination of α_c and ϕ can have a strong effect. Furthermore, it is known[6] that the airfoil section can have a strong effect in the stall region for subsonic and transonic Mach numbers. The airfoil section for the control fins is a symmetric double wedge, while the section for the wing alone used to obtain the data of Fig. 2 is a modified double wedge.

Figures 6b-d show that the correlation succeeds in taking out the ϕ dependence of the control effectiveness very well except for the bank angle region approximately ± 35 deg from the leeward plane. The ϕ dependence of Λ_{22} near the leeward plane increases with M_∞ from being hardly noticeable at $M_\infty = 2.0$ to giving Λ_{22} values different from other bank angles by more than a factor of 2 at $M_\infty = 4.5$. A check on the correlation was made for $M_\infty = 3.0$ and $\alpha_c = 35$ deg which gives a cross flow Mach number close to that for the case of Fig. 6d. The original data and the correlation are given in Fig. 7. Note that the correlation again appears to take out the ϕ dependence of Λ_{22} except for the region near the leeward plane.

The reason for the ϕ dependence of Λ_{22} near the leeward plane is not known. One possible source would be incorrect local flow field properties given by the Euler solver. For this study the radial grid points were evenly spaced between the body and the bow shock, giving a fairly coarse mesh for the leeward side at high angles of attack.

Implications for the α_{eq} Concept

From the discussion in the section above, it is clear that the α_{eq} concept as outlined in Ref. 3 will not predict control effectiveness accurately for cross-flow Mach numbers greater than 0.5. However, with a reasonable amount of effort, the method can be extended so that it can still be used successfully in missile aeroprediction codes.

To extend the concept to cross flow Mach numbers greater than 0.5, a table of $\bar{q}_\ell/q_\infty$ and $\bar{M}_\ell$ as functions of M_∞, α_c, ϕ,

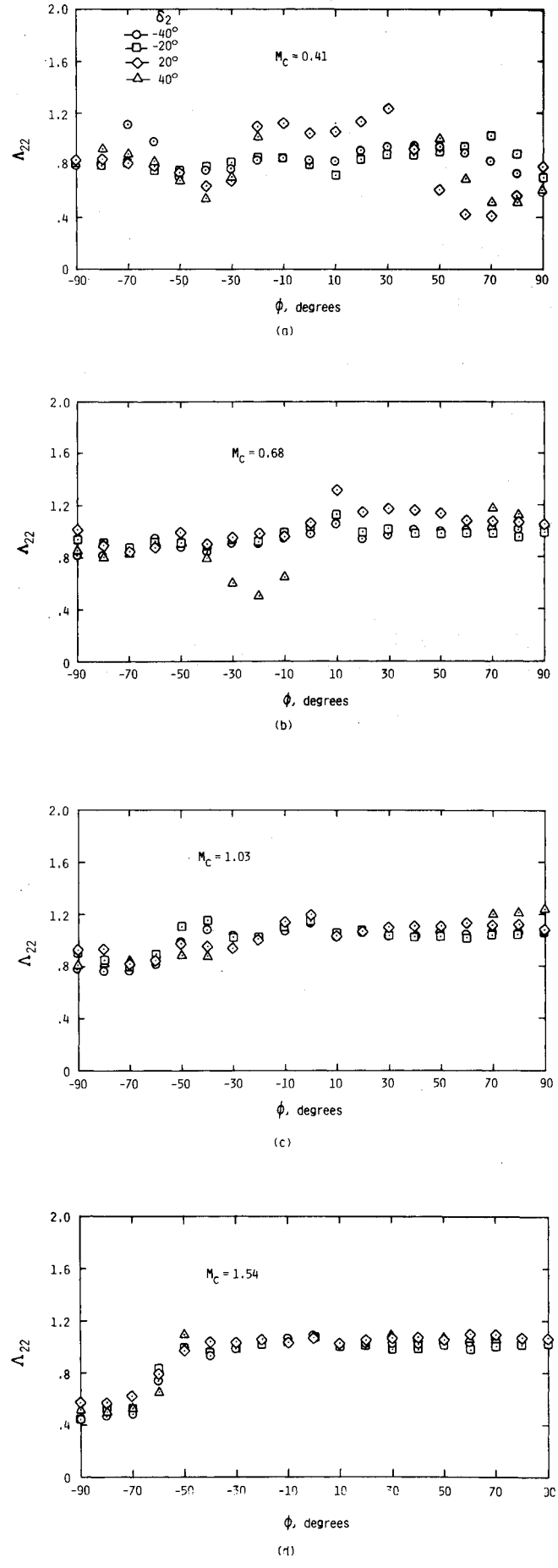

Fig. 6 Correlation of control fin effectiveness data of Fig. 3: a) $M_\infty = 1.2$; b) $M_\infty = 2.0$; c) $M_\infty = 3.0$; d) $M_\infty = 4.5$.

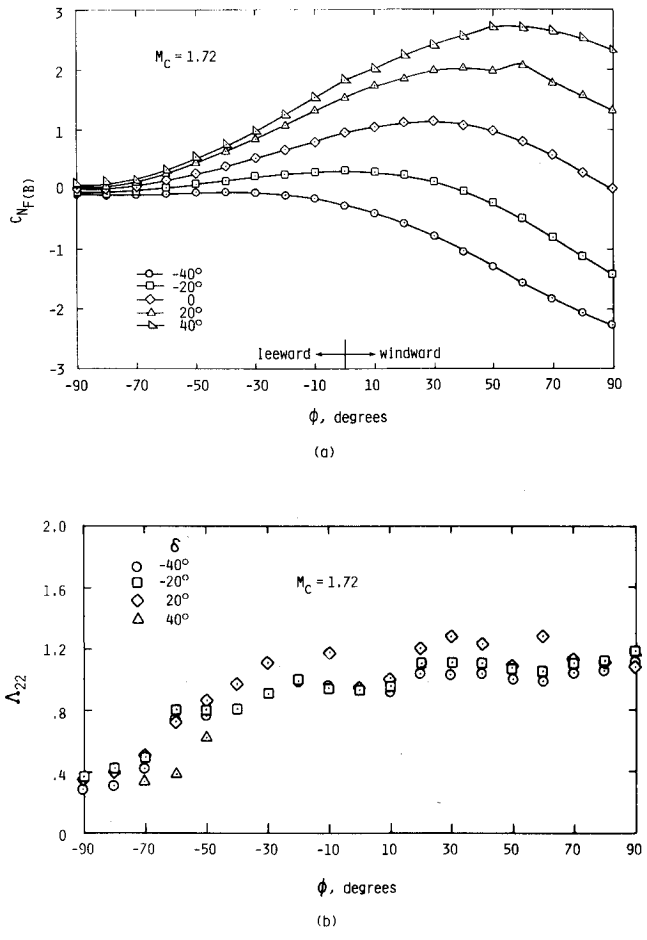

Fig. 7 Correlation of fin effectiveness data for $M_\infty = 3.0$, $\alpha_c = 35$ deg case; $AR = 2$, $\lambda = 1/2$: a) fin normal-force coefficient; b) control effectiveness.

a/s_m and x/D must be provided. Such a table can be obtained relatively inexpensively from SWINT or some other Euler solver applied to a body alone. For a missile aeroprediction method which uses a wing-alone procedure for determining fin loads (e.g., Ref. 11) the following steps should be applied:

1) Use Eqs. (2) and (3) to obtain an estimate for α_{eq} for a given $M_\infty, \alpha_c, \phi, \delta$ combination.

2) Determine $\bar{q}_\ell/q_\infty$ and $\bar{M}_\ell$ for the ϕ and x/D locations of interest.

3) Compute C_{N_W} for the α_{eq} of step 1 using the wing-alone curve for the $\bar{M}_\ell$ of step 2.

4) Multiply the C_{N_W} of step 3 by the $\bar{q}_\ell/q_\infty$ from step 2 to obtain the fin normal-force coefficient referenced to freestream conditions.

Whenever extrapolating from an experimental fin-on-body data base to different values of a/s_m, x/D and/or $(\Delta\alpha)_{v_i}$ is required, the following steps should be applied.

1) For the $M_\infty, \alpha_c, \phi, \delta$ combination of interest, determine $C_{N_{F(B)}}$ from the data base.

2) Determine $\bar{q}_\ell/q_\infty$ and $\bar{M}_\ell$ for the ϕ location of interest for the a/s_m and x/D of the fin in the data base.

3) Divide the $C_{N_{F(B)}}$ of step 1 by the $\bar{q}_\ell/q_\infty$ from step 2 to normalize it properly for use in the α_{eq} method.

4) For the wing-alone curve corresponding to the $\bar{M}_\ell$ of step 2, obtain α_{eq} for the normal-force coefficient resulting from step 3.

5) Using Eqs. (3) and (4) (see Ref. 3), determine the new α_{eq} for the conditions of interest.

6) Determine $\bar{q}_\ell/q_\infty$ and $\bar{M}_\ell$ for the ϕ value of interest for the a/s_m and x/D of interest.

7) For the α_{eq} of step 5 determine the C_{N_W} corresponding to the $\bar{M}_\ell$ of step 6.

8) Multiply the C_{N_W} of step 7 by the $\bar{q}_\ell/q_\infty$ of step 6 to get the $C_{N_{F(B)}}$ of interest referenced to freestream conditions.

Concluding Remarks

Analysis of the data from a recent comprehensive control-effectiveness test clearly shows that control effectiveness is a strong function of the local dynamic pressure and local Mach number generated by the body alone for cross-flow Mach numbers above 0.5. The analysis also suggests a simple but effective way to modify the α_{eq} concept to account for the above behavior.

The implications for various missile aeroprediction methods are important. For engineering codes which depend on data bases, the α_{eq} concept must be modified as described in the text and a data base for q_ℓ and M_ℓ included. For paneling methods linear theory will not give the full effect of compressibility. Any method which seeks to extend the linear theory so that paneling codes can be used for high angle-of-attack, high M_∞ conditions should incorporate some means of accounting for nonlinear compressibility effects in the flowfield. For finite difference codes, it is important that flowfield properties be computed accurately so that fins are immersed in the correct flow.

Acknowledgments

This work was supported in part by the Office of Naval Research, the Naval Surface Weapons Center, the Naval Air Systems Command, the Air Force Wright Aeronautical Laboratories, the Air Force Armament Test Laboratory, the Army Missile Command, and NASA Langley Research Center. The authors also gratefully acknowledge the assistance of Mr. David S. Shaw of NASA Langley Research Center, without whom there would have been no data to analyze.

References

[1]Hemsch, M.J., Nielsen, J.N., Smith, C.A., and Perkins, S.C., Jr., "Component Aerodynamic Characteristics of Banked Cruciform Missiles with Arbitrary Control Deflections," AIAA Paper 77-1153, Aug. 1977.

[2]Smith, C.A., Nielsen, J.N., and Hemsch, M.J., "Prediction of Aerodynamic Characteristics of Cruciform Missiles to High Angles of Attack," AIAA Paper 79-0024, Jan. 1979.

[3]Hemsch, M.J. and Nielsen, J.N., "Equivalent Angle-of-Attack Method for Estimating Nonlinear Aerodynamics of Missile Fins," *Journal of Spacecraft and Rockets*, Vol. 20, Jul.-Aug. 1983, pp. 356-362.

[4]Stoy, S.L. and Vukelich, S.R., "Extension of the Equivalent Angle of Attack Prediction Method," AIAA Paper 84-0311, Jan. 1984.

[5]Hemsch, M.J. and Nielsen, J.N., "Triservice Program for Extending Missile Aerodynamic Data Base and Prediction Program Using Rational Modeling," Third Annual Report, Nielsen Engineering & Research, Inc. TR 305, Aug. 1983.

[6]Nielsen, J.N. and Goodwin, F.K., "Preliminary Method for Estimating Hinge Moments of All-Movable Controls," TR 268, Nielsen Engineering & Research, Inc., Mar. 1982.

[7]Hoerner, S.F., *Fluid-Dynamic Drag*, published by the author, 1965.

[8]Wardlaw, A.B., Baltakis, J.P., Solomon, J.M., and Hackerman, L.B., "An Inviscid Computational Method for Tactical Missile Configurations," NSWC TR 81-457, Dec. 1981.

[9]Klopfer, G.H., Kuhn, G.D., and Nielsen, J.N., "Euler Solutions of Supersonic Wing-Body Interference at High Incidence Including Vortex Effects," AIAA Paper 83-0460, Jan. 1983.

[10]Landrum, E.J. and Babb, C.D., "Wind-Tunnel Force and Flow-Visualization Data at Mach Numbers from 1.6 to 4.63 for a Series of Bodies of Revolution at Angles of Attack from −4° to 60°," NASA TM 78813, Mar. 1979.

[11]Vukelich, S.R. and Jenkins, J.E., "Evaluation of Component Buildup Methods for Missile Aerodynamic Predictions," *Journal of Spacecraft and Rockets*, Vol. 19, Nov.-Dec. 1982, pp. 481-488.